Lateral offset stacked channels (LOSCs) simulations using a pseudo-genetic approach

Dimitri D'Or, Richard Labourdette and Pierre Biver

Abstract In turbidite settings, lateral offset stacked channel sand bodies (LOSCs) stack laterally and vertically as a function of turbidite story confinement degree: higher the confinement degree, lower the lateral movement and higher the vertical-to-horizontal movement ratio. A pseudo-genetic approach is proposed to simulate such stacks of channels. A B-spline is used to model the most recent channel. Previously deposited channels are then simulated by moving the B-spline control points laterally and vertically along parabolic trajectories towards the fairway's centerline and upstream. The parameters guiding the simulation are made stochastic in order to be able to explore the uncertainty about the channel deposition sequence. The generated B-splines are finally turned into channels by translating a user-defined cross-section all along the curve. Strong advantages of the method are that (i) it is able to produce realistic channel deposition sequences for a wide variety of fairway characteristics, (ii) it ensures the consistency between the individual channels, and (iii) it can be conditionned to well data.

1 Introduction

Highly sinuous deep-water channels are common in the subsurface and are important exploration targets [6]. The diversity of the architectural element organization within turbidite complex stories can complicate many aspects of hydrocarbon devel-

Dimitri D'Or
Ephesia Consult SA, 9 rue Boissonnas, CH-1227 Geneva, Switzerland, e-mail: dimitri.dor@ephesia-consult.com

Richard Labourdette
TOTAL SA, CSTJF, Avenue Larribau, 64000 Pau, France, e-mail: richard.labourdette@total.com

Pierre Biver
TOTAL SA, CSTJF, Avenue Larribau, 64000 Pau, France, e-mail: pierre.biver@total.com

Ninth International Geostatistics Congress, Oslo, Norway, June 11. – 15., 2012

opment planning, such as reservoir modeling, well design and development concept selection [3, 11, 12].

Heterogeneities result in an overall permeability anisotropy linked with individual channel stacking patterns [3, 11, 9, 15, 16]. It is by observing reservoir facies and stacking patterns in turbidite channel story complexes that the effect of heterogeneities can be assessed. The significance of barriers, baffles and overall anisotropy can be evaluated during the appraisal stage of a field by traditional methods such as high quality seismic, wells with cores, well tests and interference tests.

The turbidite stories are generally 10s meters thick. Each story consists in the evolution of an individual channel, characterized by both swing (i.e. meander loop expansion) and sweep (i.e. down system meander loop migration). Another common characteristic of channels is the dramatic stacking pattern variation over short distances along the axis (i.e. within the area of a field) [13, 14, 17]. These variations can also be observed in each channel story composing channel complexes.

The data analysis proposed is based on geometrical laws derived from seismic measurements. Eighty individual channels, from eight turbidite complexes in West Africa (upper Oligocene to Pleistocene), were studied in order to characterize their distribution patterns and define simple geometrical algorithms. The data analysis approach is based on the evolution of channel migration character and channel story characteristics. This approach allows the quantification of individual channel migrations including lateral, down-dip and vertical components.

2 Methods

The proposed simulation method can be decomposed in two main steps: calibration and simulation. At the calibration step, the limits of the fairway are digitalized as well as the last deposited channel of the sequence. Then the centerline of the fairway is computed automatically. At the simulation step, the simulation is performed using some additionnal parameters. Details of the procedure are given in this section.

2.1 Defining the fairway and computing its centerline

The channel fairway is interpreted on high-resolution seismic images. The left and right borders are digitalized (Figure 1A). Then, the centerline of the fairway is constructed as the series of points on a fine grid where the combined distance d to the borders is minimum, d being given by

$$d = \frac{\min(d_L)}{\min(d_L) + \min(d_R)}, \tag{1}$$

where $\min(d_L)$ is the minimum distance from a given grid node to the left border.

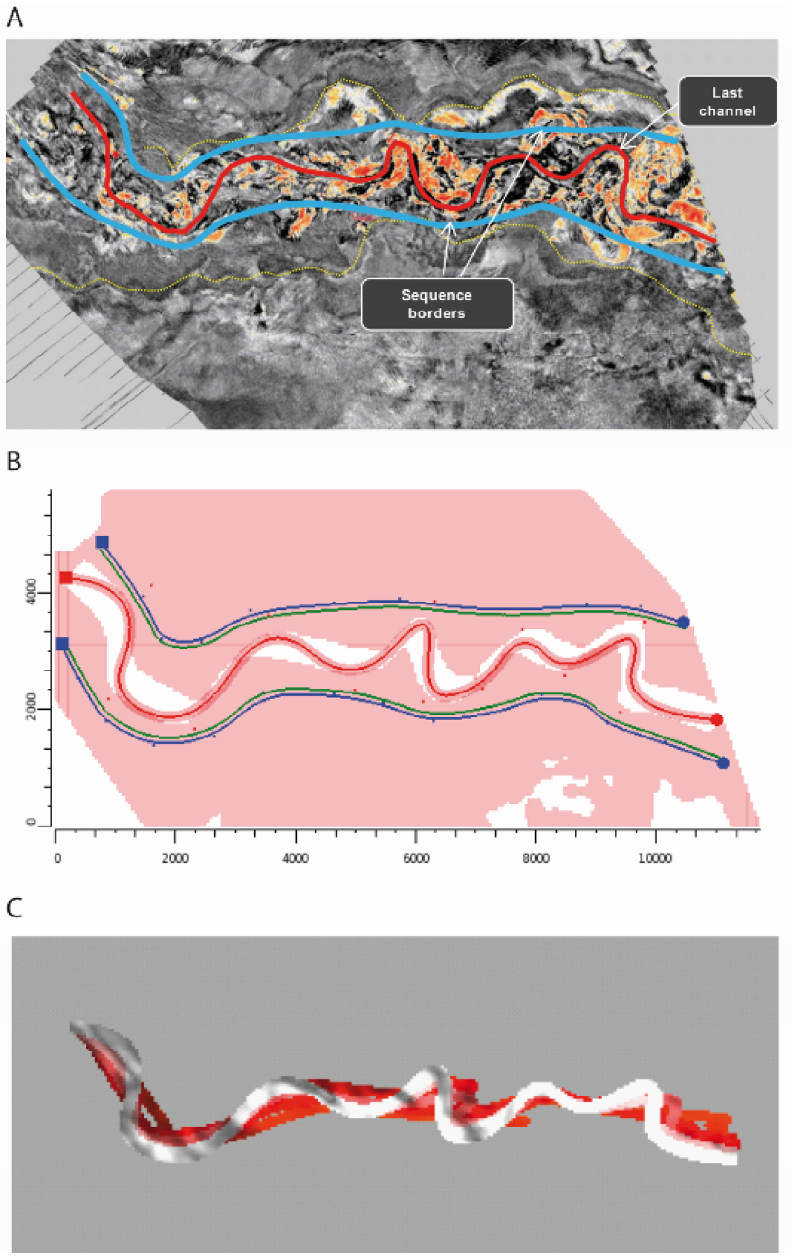

Fig. 1 Example of the workflow applied to a case study. (A) Seismic interpretation on the location of the last channel and the boders of the studied turbidite sequence. (B) Simplification of the interpretation using B-Splines to characterize characteristic points. (C) Simulation of the previous channels of the succession, using characteristic points and the given confinement degree.

2.2 Representing a channel by a B-spline

A channel can be represented by a backbone and a cross-section. The channel object is constructed by positioning the cross-section perpendicularly to the backbone and translating it all along the backbone. The backbone itself may be represented by a B-spline.

A B-spline is a piecewise curve with each component being a curve of degree p. B-splines are parameterized by a suite of control points, thus offering a very simple and powerful way to design complex shapes with lower degree polynomials. They are constructed as a series of joined Bézier curves [1, 2]

The most recently deposited channel can thus be easily digitalized from a high-resolution seismic image by only positioning adequately a set of control points (Figure 1B).

2.3 Moving the control points laterally and vertically

Analysing a sequence of channels in inverse chronological order, [8, 10] shows that each control point is following a parabolic trajectory towards the fairway centerline, vertically downwards and upstreams (Figure 2). This movement can thus be decomposed into a horizontal and a vertical parabolic trajectory. In addition, he demonstrates that the horizontal parabola stretching factor is inversely proportional to the lateral distance from the control point to the fairway centerline (Figure 3) and is also function of the confinement degree of the fairway, which is estimated as the average ratio between the fairway's depth and witdh. Vertically, the stretching factor of the parabola is dependent on the horizontal stretching factor and on the confinement degree of the channel story.

Note that in the following detailed explanations, the procedure is repeated for each control point individually, taking into account its own distance to the centerline.

2.3.1 Lateral movement

Plotting the horizontal parabola stretching factor s_h versus the lateral distance d separating a control point from the fairway's centerline for a number of channels classified into erosive or depositional fairways produced two kernel smoothed bivariate diagrams (Figure 4).

Then, for a given control point characterised by a distance d and observed in a fairway with confinement degree c, its stretching factor can be computed as follows:

1. First, knowing d, a value for s is drawn in the corresponding conditional distribution extracted from the diagram. Thus, a value $s_{h,e}$ is obtained for erosive fairways and a value $s_{h,d}$ for depositional ones.

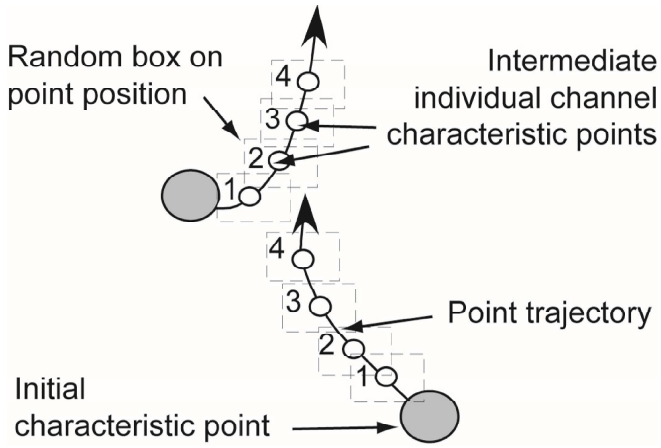

Fig. 2 Parabolic movement of the control points.

2. Second, knowing the confinement degree c, the final value for s_h is computed by linear interpolation:

$$s_h(c) = s_{h,d} + (c - 0.02)\frac{s_{h,e} - s_{h,d}}{0.25 - 0.02} \tag{2}$$

with 0.25 and 0.02 being the confinement degrees for fairways considered as the most erosive and the most depositional, respectively.

A parabola is then drawn using the control point stretching factor. The origin of the parabola correspond to the location of the control point and the axes give its relative displacement into the lateral and longitudinal directions. To bound the parabola, an arbitral superior bound is placed at 80% of the distance between the control point and the fairway's centerline. The parabola trajectory is then divided in n segments of equivalent curvilinear length (Figure 5), where n is the number of channels to simulate. The coordinates of each of the n such defined nodes give the relative displacement of the original node into the lateral and longitudinal directions.

To add some randomness to the process, an uncertainty may be put on the stretching factor, thus delimiting an area around the parabola. Around each segment node, a box fitting this area can be constructed, wherein the actual node can be drawn randomly. This uncertainty is given as a percentage p and is used to compute confidence interval curves around the parabola with

$$y_{inf} = (s - p)x^2 \tag{3}$$

$$y_{sup} = (s + p)x^2 \tag{4}$$

At any location x along the parabola, the size of the bounding box is given by :

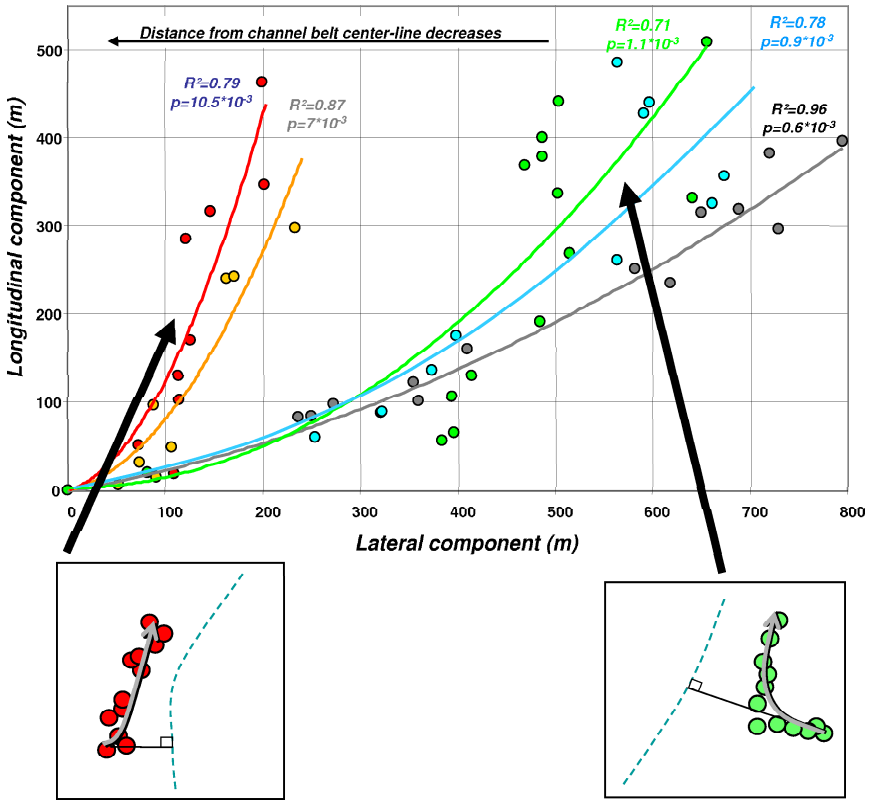

Fig. 3 Parabolic movement of the control points. All the control points of a given channel are depicted in the same color. The relationship between the movement towards the fairway centerline and the upstream movement is a parabola. The parabola stretching factor is porportional to the lateral distance of the control point of the most recent channel to the fairway centerline. (Source : [8]).

$$t_x = \sqrt{\frac{y}{s-p}} - \sqrt{\frac{y}{s+p}} \tag{5}$$

$$t_y = 2px^2 \tag{6}$$

It is thus a rectangle of size $[t_x;t_y]$ centered on the point (x,y) (Figure 5).

As an additional refinement, the random draw of the segment nodes in their bounding box along the parabola can be made more of less correlated. To achieve this task, deviations along the X and Y axes are generated using a sequential gaussian simulation. The spatial correlation is defined by a Gaussian variogram with range set equal to ρ, where ρ is the correlation percentage given as parameter. Setting $\rho = 1$ generates perfectly correlated relative deviations in the bounding boxes, while $\rho = 0$ results in totally uncorrelated deviations.

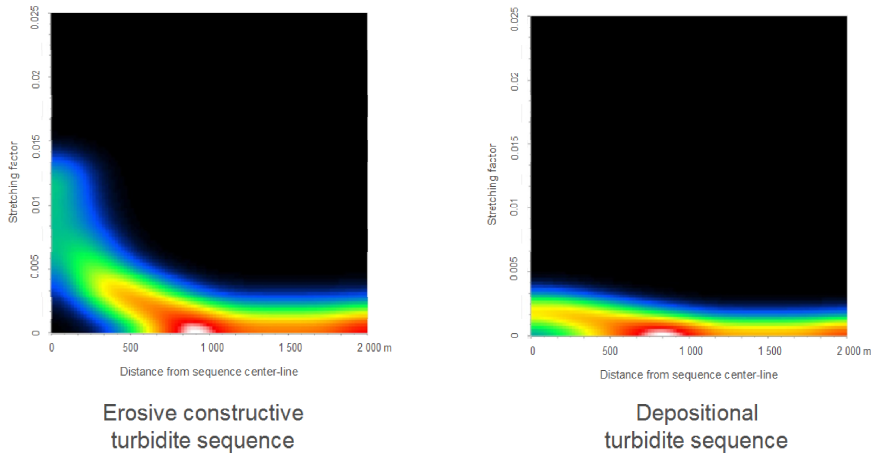

Fig. 4 Kernel smoothed plots representing the horizontal parabola stretching factor s_h versus the lateral distance d separating a control point from the fairway's centerline for a number of channels classified into erosive (left) or depositional (right) fairways.

2.3.2 Vertical movement

The vertical displacement of a control point can be expressed as a function of the confinement degree of the channel story using the following relation [10]:

$$\bar{d}_v = (0.016 + 0.8c)\bar{d}_h \tag{7}$$

where $\bar{d}_v$ is the average vertical displacement along the channel and c is the confinement degree. The value of $\bar{d}_h$ is the average curvilinear distance along the parabola in the horizontal plane, computed as the average curvilinear distances for all de control points. The values of the intercept (0.016) and the slope (0.8) are the result of the data analysis of a dozen of channel stories. Based on additional analyses, these values may be revised.

2.4 Conditioning to well data

If well data are avalaible, they may be taken into account in the simulation process. First, facies are classified as belonging to the channel or not. Channels should pass through wells wherein channel facies were observed, while they should avoid wells with matrix facies.

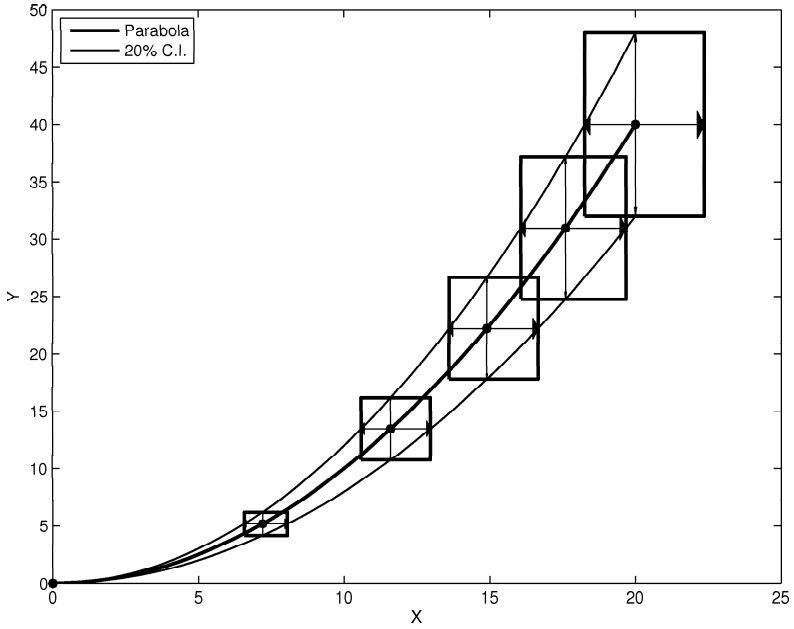

Fig. 5 Parabola for computing the relative lateral and longitudinal movements of the control point. The parabola is surrounded by a given confidence interval. Curvilinear equidistant points are represented by black circles. Around them are built the bounding boxes inside which the points are randomly drawn with more or less correlation among them.

Conditioning may be realized prior or posterior to the channel simulation. In this case, it was easier to condition simulation *a posteriori*, i.e. to modify a channel trajectory to force it to pass or to avoid a well. To achieve this goal, B-splines representing the channel backbone are converted into Piecewise Polynomial Cubic Splines (PPCS). Those curves have the advantage to be parametrized by control points positioned on the curve.

Two categories of points belong to the PPCS control points list: (list A) the points on the curve that are located the nearest to the B-spline control points and (list B) the inflexion points found in each segment delimited by the points of list A.

Once this list has been built, the conditioning data are examined one after the other. For a given data, it is first tested if it is honored. If not, the nearest point on the PPCS is searched. Let us denote this point by x and the distance beween it and the data by d. Two cases can occur:

1. The data point must be inside the channel but is not. The point x is then moved towards the data point so that it comes at a distance equal to uw, where u is a random number between 0 and 1, and w is the half width of the channel.

2. The data point is inside the channel while it should not. The point x is then moved perpendicularly to the channel backbone in the opposite direction of the data point by a distance $u(w+d)$.

2.5 Turning the channel backbone into a channel object using the cross-section

Once the channel backbones have been drawn and conditioned to the well data, the channels are built around them. For this purpose, the user-designed cross-section is positionned perpendicularly to the backbone and translated all along the channel. This cross-section may be multi-facies.

2.6 Summary of the simulation algorithm

As a summary, the simulation process may be divided in two major steps: calibration and simulation. At the calibration step, the fairway borders and the last channel backbone are digitalized from high resolution seimsic images, the fairway centerline is computed and the (possibly multi-facies) cross-section is drawn. The additional parameters needed for the simulation are the number of channel to draw (possibly a random number drawn from a Poisson or user-defined distribution), the confinement degree and the parabola uncertainty factor. The simulation generates a set of channel objects that may be rasterized to yield a gridded property.

3 Illustration

This case study example is composed of three main turbidite sequences cutting each others. The classical workflow consists in interpreting each sequence separately. As in Figure 1A, seismic attribute maps are used to locate the last channel and the borders of the studied turbidite sequence. This interpretation is integrated within the software module and picked lines are transformed using B-Spline, to simplify their representation and identify characteristic points (Figure 1B). By using this interpretation coupled with the associated confinement degree, the previous channels of the succession are simulated to obtain the complete infill of the turbidite sequence (Figure 1C). In this example, a succession of three main sequences was identified. They are simulated separately and merged together at the end of the workflow, allowing multiple erosions of the simulated channels. The resulting reservoir image is realistic and in accordance with the pattern observed on seismic attributes (Figure 6).

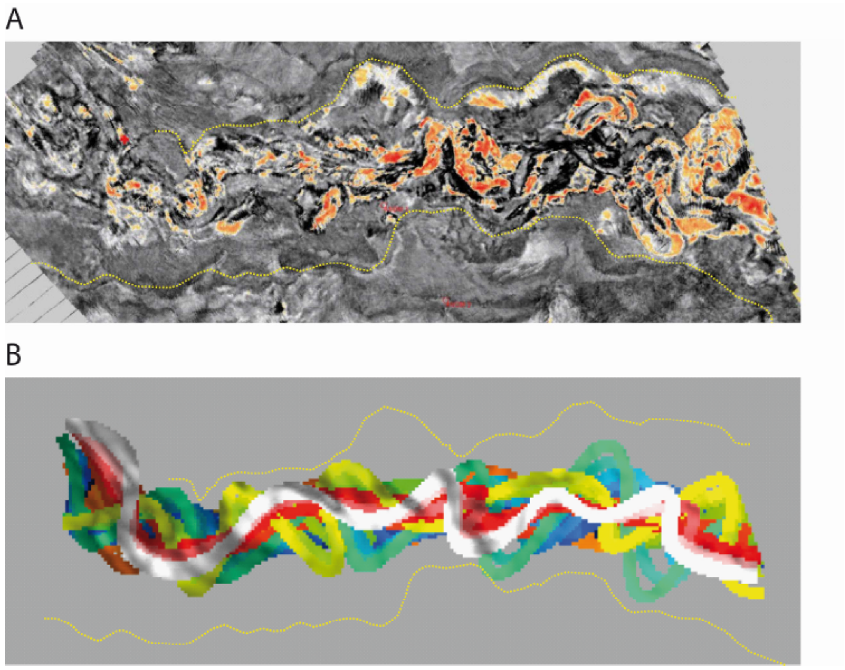

Fig. 6 Comparison of seismic attributes (A) and the final representation of the three identified turbidite sequences (B). The position of the lateral migrating channels is consistent with the observations.

4 Conclusion

Strongly inspired by the observed evolution of channel trajectories with time, the proposed pseudo-genetic object simulation method ensures that the channels have a natural aspect. It guarantees also that the various channels in a sequence are coherent with each other, evolving by progressive migration laterally and/or downdip. Randomness is added in the process by the way of several parameters allowing to explore the uncertainty about the channel deposition process. Finally, simulations can be conditioned to facies data observed in wells.

Further developments will include the possibility to let the confinement degree vary along the fairway story and improvements in the data conditioning approach, which can be put in difficulties when abundant data are available.

Acknowledgements The authors would like to acknowledge R. Froidevaux (Ephesia Consult) for positive discussions and debates on this subject and Total SA for sponsoring this research and allowing this publication.

References

1. Bézier, P. (1968). How Renault uses numerical control for car body design and tooling. Society for Automotive Engineers, Paper SAE 6800010.
2. Bézier, P. (1993). The First Years of CAD/CAM and the UNISURF CAD System. *In: Fundamental Developments of Computer-Aided Geometric Modeling*, (ed. L. Piegl) (Academic Press).
3. Clark, J. D. and Pickering, K. T. (1996). Architectural elements and growth patterns of submarine channels; application to hydrocarbon exploration: American Association of Petroleum Geologists Bulletin, **80**, 194–221.
4. Cox, M. (1972). The Numerical Evaluation of B-splines. *J. Inst. Math. Appl*, **10**, 134–149.
5. De Boor, C. (1972). On calculating with B-splines. *J. Approx. Theory*, **6**, 50–62.
6. Kolla, V. and Bourges, P and Urruty, J. M. and Safa, P. (2001). Evolution of Deep-Water Tertiary Sinuous Channels Offshore Angola (West Africa) and Implications for Reservoir Architecture: American Association of Petroleum Geologists Bulletin, **85**, 1373–1405.
7. Labourdette R. (2007). Laterally Offset Stacked Channels Simulations: Toward geometrical modeling of turbidite elementary channels. In: AAPG Conference 2007.
8. Labourdette R. (2008). 'LOSCS' Lateral Offset Stacked Channel Simulations: Towards geometrical modelling of turbidite elementary channels. Basin Research **20**(3), 431–444.
9. Labourdette, R. and Poncet, J. and Seguin, J. and Temple, F. and Hegre, J. and Irving A. (2006). Three-dimensional modelling of stacked turbidite channels in West Africa: impact on dynamic reservoir simulations: Petroleum Geoscience, **12**, 335–345.
10. Labourdette R. and Bez M. (2010). Element migration in turbidite systems: Random or systematic depositional processes? AAPG Bulletin **94**(3), 345–368.
11. Mayall, M. and O'Byrne, C. J. (2002). Reservoir prediction and development challenges in turbidite slope channels: Offshore Technology Conference, p. OTC n° 14029.
12. Mayall, M. and Jones, E. and Casey, M. (2006). Turbidite channel reservoirs–Key elements in facies prediction and effective development: Marine and Petroleum Geology, **23**, 821–841.
13. Peakall, J., B. McCaffrey, and B. Kneller (2000). A Process Model for the Evolution, Morphology, and Architecture of Sinuous Submarine Channels: Journal of Sedimentary Research, **70**, 434–448.
14. Posamentier, H. W., (2003). Depositional elements associated with a basin floor channel-levee system: case study from the Gulf of Mexico: Marine and Petroleum Geology, **20**, 677–690.
15. Stright, L. and Caers, J. and Li, H. and Van Der Vlugt, F. and Pirmez, C. and Barton, M. (2006). Modeling, upscaling and history matching thin, irregularly-shaped flow barriers: a comprehensive approach for predicting reservoir connectivity: 26th Annual GCSSEPM Foundation Bob F. Perkins Research Conference - Reservoir Characterization: Integrating Technology and Business Practices, p. 985–1002.
16. Weimer, P., and R. M. Slatt (2007). Petroleum Geology of Deepwater Settings: AAPG Studies in Geology, **57**: Tulsa, American Association of Petroleum Geologists, 816 p.
17. Wynn, R. B., B. T. Cronin, and J. Peakall, (2007). Sinuous deep-water channels: Genesis, geometry and architecture: Marine and Petroleum Geology, **24**, 341–387.